ABSOLUTE STRESS DETERMINATION FROM ANGULAR DEPENDENCE OF ULTRASONIC VELOCITIES IN ORTHOTROPIC MATERIALS

A. D. Degtyar and S. I. Rokhlin
The Ohio State University
Nondestructive Evaluation Program
Columbus, Ohio 43210

INTRODUCTION

The characteristic dependence of ultrasonic velocity on stress has for a long time been thought a promising for making residual stress measurements in materials. For a review of theory and experimental methods the reader is referred to [1–3]. Different wave modes were proposed for stress determination. Through-thickness average stress can be obtained using longitudinal wave data at normal incidence [4, 5] or transverse waves with different polarizations [6–8]. Near-surface stresses can be determined using Rayleigh waves [9–11] and surface-skimming longitudinal [12] and SH [12, 13] waves.

It is now well understood that there are complications in the practical utilization of the ultrasonic stress measurement technique. First of all velocity changes due to stress are small (typically below 0.1%) and very precise measurements of the time delay and travelling distance are required. However the major difficulty is the necessity of separating the effects of texture (anisotropy) and stress on the measured ultrasonic velocity. In most cases materials under consideration have unknown anisotropy and even if the anisotropy is small its effect cannot be neglected in stress measurements. Several methods have been proposed to overcome this difficulty. Thompson et al. [12] consider the difference of two SH-waves propagating in the plane of the material in orthogonal directions. They showed that for this difference the effect of anisotropy is reduced by an order of magnitude and for small anisotropy it can be neglected. Also they demonstrate that the stress and anisotropy terms have different angular dependences which can be used for their separation. King and Fortunko [6] considered obliquely incident SH-waves. Again a formula was derived with separate anisotropic and stress terms. Man and Lu [14] generalized both techniques and demonstrated the applicability of the ultrasonic method for stress measurements in materials which had undergone a complicated (possibly plastic) history of loading and unloading. Generalizing Thompson's results, they obtained relations between certain combinations of stresses and velocities which do not include elastic constants and thus are independent of initial texture and change of microstructure due to plastic deformations.

In this paper we will show that stresses in a material can be found simultaneously with stress–dependent elastic constants from the inversion of the Christoffel equation, using as input measured angular dependencies of ultrasonic velocities. The method is applicable for determination of both applied and residual stresses for materials of the

Review of Progress in Quantitative Nondestructive Evaluation, Vol. 14
Edited by D.O. Thompson and D.E. Chimenti, Plenum Press, New York, 1995

most general loading histories, in line with the discussion of Man and Lu [14]. Simulation results are presented for orthotropic media to validate this technique. We will show that the absolute error in stress determination using this technique is independent of the degree of anisotropy and the stress level is defined only by the accuracy of wave velocity measurement.

CHRISTOFFEL EQUATION IN STRESSED MEDIA

To describe the wave propagation in a prestressed medium we use the approach proposed by Man and Lu [14]. The prestressed configuration is the only reference configuration in this approach and the initial stress is included in the constitutive equation:

$$\mathbf{S} = \mathbf{\Sigma} + \bar{\mathbf{C}} : \mathbf{E} + \mathbf{H}\mathbf{\Sigma} \tag{1}$$

where $\mathbf{S}$ is the first Piola-Kirchhoff stress, $\mathbf{\Sigma}$ is the initial stress, $\mathbf{E}$ is the elastic strain due to wave propagation, $\mathbf{H}$ is the displacement gradient and $\bar{\mathbf{C}}$ is the fourth rank tensor of stress dependent elastic constants. The equation for small elastic motion due to wave propagation superimposed on the prestressed state is:

$$\nabla \cdot \mathbf{S} = \rho \frac{\partial^2 \mathbf{u}}{\partial t^2} \tag{2}$$

where $\mathbf{u}$ is the displacement vector. Making use of Eq. (1), Eq. (2) can be written in component form:

$$\frac{\partial}{\partial x_j}(\bar{C}_{ijkl} + \sigma_{jl}\delta_{ik})\frac{\partial u_k}{\partial x_l} = \rho \ddot{u}_i \tag{3}$$

The stress σ_{ij} can be both applied and residual since there is no restriction that the resulting deformation be elastic. Now assuming that the material and local (over the size of the transducer) stress are homogeneous and using a plane wave solution for $\mathbf{u}$

$$\mathbf{u} = \mathbf{p}e^{ik(\mathbf{n}\cdot\mathbf{x}-vt)} \tag{4}$$

where $\mathbf{p}$ is the unit vector in the direction of particle motion, k is the wave number and $\mathbf{n}$ is the unit vector in the direction of wave propagation, one has the Christoffel equation for an anisotropic material under stress:

$$[\bar{C}_{ijkl}n_i n_l + (\sigma_{il}n_i n_l - \rho V^2)\delta_{jk}]p_k = 0 \tag{5}$$

Eq. (5) was derived by Tokuoka and Iwashimizu [15] and used by Thompson et al. [12] and King and Fortunko [6]. Man and Lu [14] reexamined constitutive equations and extended the applicability of Eq. (5) to general types of loading history, including plastic deformations.

Eq. (5) has a convenient form for our further use. The difference from the Christoffel equation in an unstressed medium is the appearance of stress dependent elastic constants $\bar{C}_{ijkl}$ instead of second order elastic constants C_{ijkl} and the addition of the stress

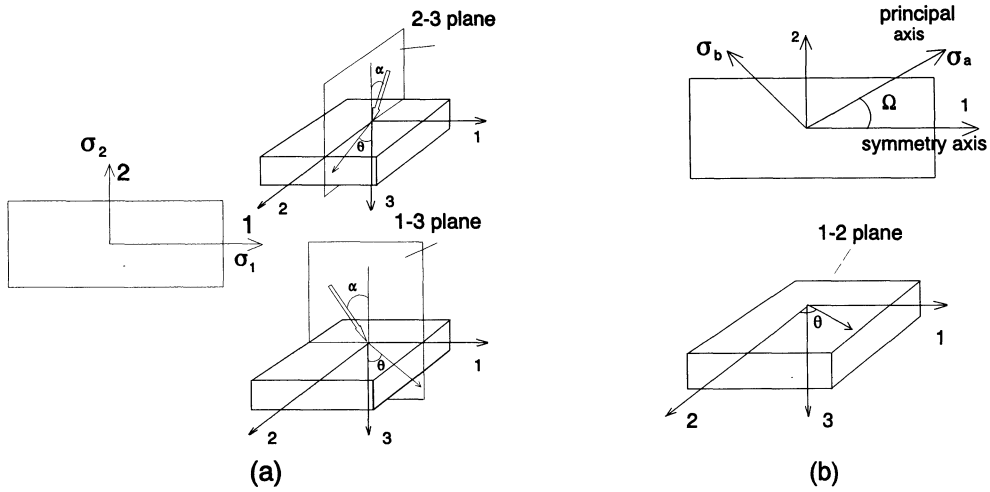

Fig. 1. (a) Principal stresses along symmetry axes in the 1-2 plane and wave propagation in the 1-3 and 2-3 symmetry planes; (b) Principal stresses off symmetry axes in the 1-2 plane and wave propagation in the plane of stresses.

term $\sigma_{il}n_in_l$ in the diagonal elements of (5). The effect of the stress term on the wave velocity can be separated off.

To validate our approach by computer simulation and to create a synthetic set of experimental data we need to be able to compute stress dependent elastic constants $\bar{C}_{ijkl}$ as a function of stress. This can be done for a finitely stressed hyperelastic body using second and third order elastic constants. While the velocity data set thus generated is for hyperelastic material, our reconstruction process, using Eq. (5), does not have this limitation and has the same applicability as Eq. (5) itself.

DEPENDENCE OF ULTRASONIC VELOCITY ON STRESS. DETERMINATION OF STRESS

We will consider two cases of principal stress orientation with respect to material axes of symmetry. When principal axes coincide with symmetry axes of the material, we analyze the propagation of quasilongitudinal (QL) and quasishear (QT) waves in symmetry planes 1-3 and 2-3 perpendicular to the symmetry plane of the material 1-2 (Fig. 1a). In the general plane stressed state, i.e. when principal directions deviate from symmetry axes, we utilize waves propagating in the plane of stress (1-2 plane) and polarized in the same plane.

Principal Stresses along Symmetry Axes

When principal axes coincide with symmetry axes of an orthotropic material, the stresses do not change the symmetry and the number of independent $\bar{C}_{ij}$ in the stressed solid is the same as the number of second order elastic constants C_{ij}. Let us consider plane stress in the 1-2 plane with the shear stress component σ_{12} being zero and wave propagation in the 1-3 or 2-3 symmetry planes (see Fig. 1a). For wave propagation in the 1-3 plane the Christoffel equation (5) has the following form:

$$\begin{vmatrix} \bar{G}_{11} - (\rho V^2 - \sigma_{11} s^2) & 0 & \bar{G}_{13} \\ 0 & \bar{G}_{22} - (\rho V^2 - \sigma_{11} s^2) & 0 \\ \bar{G}_{13} & 0 & \bar{G}_{33} - (\rho V^2 - \sigma_{11} s^2) \end{vmatrix} = 0 \qquad (6)$$

where

$$\begin{aligned} \bar{G}_{11} &= \bar{C}_{11} s^2 + \bar{C}_{55} c^2; \quad & \bar{G}_{33} &= \bar{C}_{55} s^2 + \bar{C}_{33} c^2; \\ \bar{G}_{13} &= (\bar{C}_{13} + \bar{C}_{55}) sc; \quad & \bar{G}_{22} &= \bar{C}_{66} s^2 + \bar{C}_{44} c^2; \\ s &= \sin\theta; \quad & c &= \cos\theta. \end{aligned} \qquad (7)$$

The angle θ is between the direction of propagation and the 3-axis (Fig. 1a). The equation (6) can be decoupled and simple closed-form solutions for QL and QT wave velocities are:

$$\begin{aligned} \rho V_{QL}^2 &= \frac{\bar{G}_{11} + \bar{G}_{33}}{2} + \frac{\sqrt{(\bar{G}_{11} - \bar{G}_{33})^2 + 4\bar{G}_{13}^2}}{2} + \sigma_{11} s^2 \\ \rho V_{QT}^2 &= \frac{\bar{G}_{11} + \bar{G}_{33}}{2} - \frac{\sqrt{(\bar{G}_{11} - \bar{G}_{33})^2 + 4\bar{G}_{13}^2}}{2} + \sigma_{11} s^2. \end{aligned} \qquad (8)$$

As we can see the QL and QT wave velocities in this symmetry plane depend only on five parameters, namely $\bar{C}_{11}, \bar{C}_{33}, \bar{C}_{13}, \bar{C}_{55}$ and σ_{11}. Similarly, QL and QT wave velocities in the 2-3 plane depend on four stress dependent elastic constants $\bar{C}_{22}, \bar{C}_{33}, \bar{C}_{23}, \bar{C}_{44}$ and the stress component σ_{22}.

From the angular dependence of the measured velocities we can determine these five unknown parameters for each plane separately. We employ the *least squares method* for the minimization of the sum of squared deviations between experimental and calculated, using Eq. (8), velocities considering effective elastic constants and stress component as variables in multidimensional space:

$$\min_{\bar{C}_{ij}, \sigma_{ij} \in \Re^n} \frac{1}{2} \sum_{i=1}^{m} (V_i^e - V_i^c)^2, \qquad (9)$$

where n is the number of parameters to be defined, m is the number of velocity measurements for different directions, and V^e and V^c are the experimental and calculated phase velocities, respectively. This approach was used by Chu and Rokhlin [17] and Chu et al. [18] to find second order elastic constants from velocity data in symmetry and nonsymmetry planes for orthotropic materials.

The flow chart of the inversion procedure for the 1-3 plane is presented in Fig. 2a. Four effective elastic constants ($\bar{C}_{11}, \bar{C}_{33}, \bar{C}_{13}, \bar{C}_{55}$) and one stress component (σ_{11}) form a 5–dimensional space of unknown parameters which determine the velocities of the QL and QT waves. The function to be minimized in this space is defined by the sum of squared differences between experimental and calculated velocities at different propagation angles. Thus in the inversion procedure $\bar{C}_{ij}$ and stress are considered to be

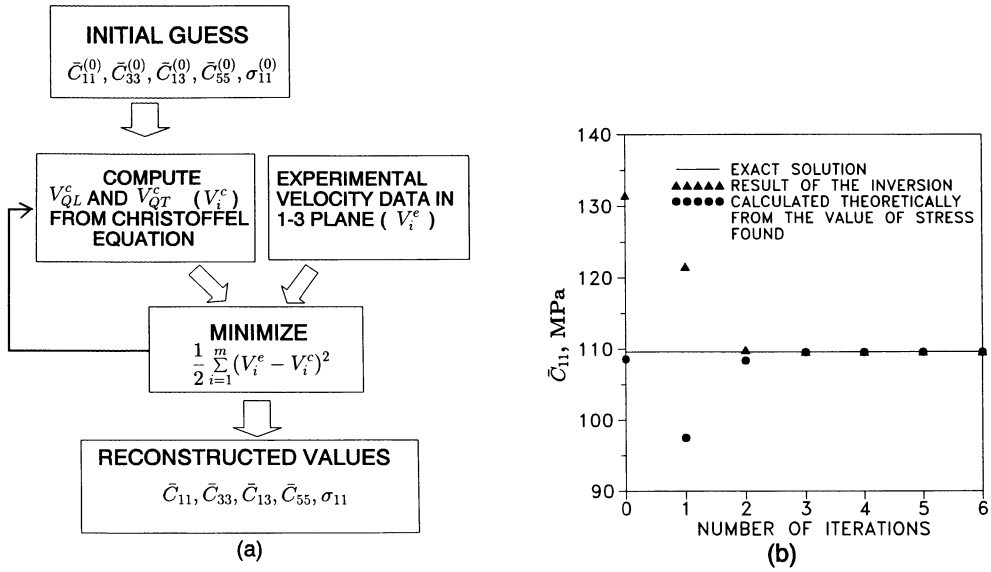

Fig. 2. (a) Scheme of the inversion procedure in 1-3 plane;
(b) Results of the inversion for $\bar{C}_{11}$ after each iteration.

independent parameters although actually $\bar{C}_{ij}$ depend on stress. To validate the procedure we checked numerically that the reconstructed values for $\bar{C}_{ij}$ have the correct dependence on the reconstructed value of stress (i.e. actual value of stress). Fig. 2b shows with triangles the results after each iteration during determination of $\bar{C}_{11}$ using nonlinear least squares minimization. The circles show the values of $\bar{C}_{11}$ calculated exactly using the stress (σ_{11}) determined at this iteration step and the second and third order elastic constants used for creation of the synthetic set of velocity data. We see that starting with the third iteration both results for $\bar{C}_{11}$ are very close to each other and to the original value (shown by the straight solid line). This shows that the correct dependence between $\bar{C}_{11}$ and σ_{11} holds for values determined from inversion although their relation is not specified in the inversion algorithm.

When the reconstruction from velocity data is performed for both the 1-3 and 2-3 planes, both stress components σ_{11} and σ_{22} and seven of nine effective elastic constants (all except $\bar{C}_{12}$ and $\bar{C}_{66}$) can be found. If $\sigma_{12} \neq 0$ then the solution of Christoffel equation in the 1-3 plane cannot be presented in the form of Eq. (8) because this shear stress component alters the material symmetry and the 1-3 plane becomes the nonsymmetry plane. As has been shown in [18] the reconstruction from a nonsymmetry plane is unstable. Our calculations show that the effect of even very small scatter in the velocity data destabilizes the inversion process for stress. More effort will needed to develop stable algorithms for this case.

Principal Stresses Off Symmetry Axes

Now let us consider an arbitrary plane stress state in the 1-2 plane (Fig. 1b), σ_{11}, σ_{22} and σ_{12} are the only nonzero stress components. In this case the symmetry reduces to monoclinic. $\bar{C}_{16}, \bar{C}_{26}, \bar{C}_{36}, \bar{C}_{45}$ are stress-induced effective elastic constants. They depend only on the shear stress component σ_{12}. Instead of considering wave propagation in planes orthogonal to the stress plane, we consider the wave propagation in the plane of the stresses (Fig. 1b). This plane still remains the plane of symmetry and the Christoffel equation (5) can again be decoupled. The solutions for quasilongitudinal and quasishear (polarized in the stress plane) waves have the following form:

$$\rho V_{QL}^2 = \frac{\bar{G}_{11}+\bar{G}_{22}}{2} + \frac{\sqrt{(\bar{G}_{11}-\bar{G}_{22})^2+4\bar{G}_{12}^2}}{2} + (\sigma_{11}-\sigma_{22})s^2 + \sigma_{22} + 2\sigma_{12}sc$$
$$\rho V_{QT}^2 = \frac{\bar{G}_{11}+\bar{G}_{22}}{2} - \frac{\sqrt{(\bar{G}_{11}-\bar{G}_{22})^2+4\bar{G}_{12}^2}}{2} + (\sigma_{11}-\sigma_{22})s^2 + \sigma_{22} + 2\sigma_{12}sc \tag{10}$$

where

$$\bar{G}_{11} = \bar{C}_{11}s^2 + \bar{C}_{66}c^2 + 2\bar{C}_{16}sc; \quad \bar{G}_{12} = (\bar{C}_{12}+\bar{C}_{66})sc + \bar{C}_{16}s^2 + \bar{C}_{26}c^2;$$
$$\bar{G}_{22} = \bar{C}_{66}s^2 + \bar{C}_{22}c^2 + 2\bar{C}_{26}sc; \quad s = \sin\theta; \quad c = \cos\theta. \tag{11}$$

We use the inversion procedure in the space of unknowns $\bar{C}_{11}, \bar{C}_{22}, \bar{C}_{12}, \bar{C}_{66}, \bar{C}_{16}, \bar{C}_{26}$, $\sigma_{11}, \sigma_{22}, \sigma_{12}$. From (10) we can see that the difference of normal stresses $\sigma_{11} - \sigma_{22}$ and shear stress σ_{12} have different angular dependences which we can determine using the inversion procedure described above.

SIMULATION RESULTS

To validate the technique described computer simulation tests were performed for materials with different degrees of anisotropy. To obtain the synthetic set of data points we assume that the second and third order elastic constants are known. For a given stressed state, $\bar{C}_{ij}$ can be found assuming that the material is hyperelastic and the velocities can be determined from the Christoffel equation (5). Different levels of random scattering are introduced into this velocity data and this data set is used for the reconstruction of effective elastic constants and stresses. The values of stress and $\bar{C}_{ij}$ found are compared with those originally selected in the simulations to determine the precision of the procedure.

First, computations were made for principal stresses along symmetry axes in the 1-2 plane and obliquely incident quasilongitudinal and quasishear waves. It was observed that the stress component σ_{22} does not affect the results of the reconstruction of σ_{11} from velocity data in the 1-3 plane. This happens because σ_{22} affects the velocity data in the 1-3 plane only through the effective elastic constants and in the reconstruction process we consider σ_{11} as an independent unknown. We present here the results for the case of uniaxial stress along the 1-axis and velocity data in the 1-3 plane. The angular range for θ we take to be close to that experimentally available using the double-through transmission technique [19] for metals. For a quasilongitudinal wave it is approximately $0° - 60°$ and for a quasishear wave $30° - 70°$. The total number of synthetic data points is 45. As an initial guess for the effective elastic constants we take the second order elastic constants found assuming no stress [17]. The initial guess for stress was set to be zero. The first material considered was textured aluminum (anisotropy was 1%). The third order elastic constants were taken from [16] for isotropic aluminum. Results of the reconstruction are presented in Table 1a. Different stress levels and different scattering are considered. The same computations were also made for a graphite/epoxy composite which exhibits strongly anisotropic properties. It was assumed that this material is orthotropic. The third order elastic constants were chosen arbitrarily assuming only that they are approximately one order of magnitude higher than the second order elastic constants. It was observed that a different choice of third order elastic constants did not affect the accuracy of the reconsruction process. The reconstruction results are presented in Table 1b.

Comparing these results we conclude that the precision of the reconstructed stress values does not depend on the degree of anisotropy. For each scattering level we have

Table 1. Results of stress reconstruction for (a) textured aluminum and (b) graphite/epoxy composite samples for different stress levels and scattering.

Original value σ_{11}, MPa	Standard deviation of the reconstructed value from the original, MPa							
	no scatter		0.01 % scatter		0.05 % scatter		0.1 % scatter	
	a	b	a	b	a	b	a	b
0	0	0	5	5	15	22	48	39
100	0	0	5	5	24	20	36	56
200	0	0	4	6	26	27	49	56
300	0	0	5	6	25	28	40	56
400		0		4		24		51
500		0		4		23		54

approximately the same absolute error in stress determination regardless of the stress level.

To consider the effect of error in the velocity data we introduced different levels of scattering in synthetic velocity data using a random function generator. We changed the scattering from zero to 0.1% and reconstructed the known value of stress for anisotropic aluminum. The results are presented in Fig. 3a for the case of applied tensile stress equal to 100 MPa. For each scattering level we made 50 runs of the reconstruction program with different synthetic data. We see that upon increasing the scattering from 0.01% to 0.1% the accuracy drops by a factor of roughly ten. Fig. 3b represents the distribution of reconstructed values of stress for the case of applied stress 100 MPa and scattering 0.02% (total number of runs = 1000). The distribution obtained can be approximated by a normal distribution with deviation $\sigma = 6.58$. So the results of the theory of probability for the normal distribution are applicable in our case.

SUMMARY

An approach for absolute stress determination from angular dependence of ultrasonic velocities has been described. It is based on inversion of the Christoffel equation in a multidimensional space formed by effective elastic constants and stress components. The technique is applicable for determination of both applied and residual stresses. In the case when principal plane stress directions coincide with symmetry axes of the orthotropic material, one can reconstruct principal stresses from the angular dependence of quasilongitudinal and quasishear waves measured in these planes. When the principal axes do not coincide with symmetry axes the angular dependence of quasilongitudinal and quasishear waves propagating and polarized in the plane of stresses can be used to determine the difference between normal stress and shear stress components. Numerical simulation has been performed using a set of synthetic velocity data from all three symmetry planes. The reconstructed values are not affected by the selection of the initial guesses. The results show that the absolute error in stress determination does not depend on the stress level and the degree of anisotropy of the material.

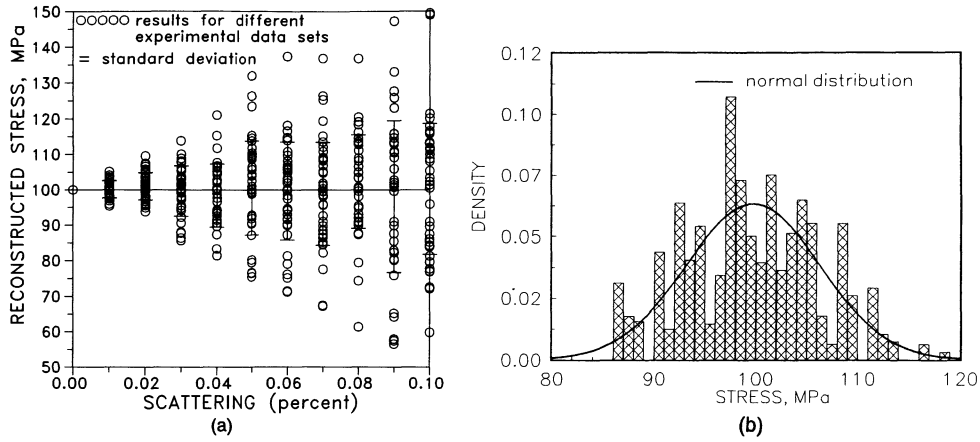

Fig. 3. (a) Results of stress reconstruction for anisotropic aluminum under applied tensile stress of 100 MPa from velocity data with different scattering; (b)Distribution of reconstructed values of stress for different synthetic data. Applied tensile stress is 100 MPa and scattering is 0.02%.

REFERENCES

1. Y. H. Pao, W. Sachse and H. Fukuoka, in *Physical Acoustics*, Vol. 17, eds. W. P. Mason and R. N. Thurston (Academic, New York, 1984), Chap.2.
2. J. H. Cantrell and K. Salama, International Materials Reviews 36, 125 (1991).
3. R. B. Thompson, W.-Y. Lu and A. V. Clark, Jr., in *SEM Monograph of Techniques for Residual Stress Measurement*, (in preparation), Chap.7.
4. J. J. Dike and G. C. Johnson, J. Appl. Mech. 57, 12 (1990).
5. G. S. Kino, J. B. Hunter, G. C. Johnson, A. R. Selfridge, D. M. Barnett, G. Hermann and C. R. Steele, J. Appl. Phys. 50, 2607 (1979).
6. R. B. King and C. M. Fortunko, J. Appl. Phys. 54, 1339 (1983).
7. A. V. Clark, J. C. Moulder, R. B. Mignogna and P. P. Delsanto, in *Review of Progress in Quantitative NDE*, Vol. 5B, eds. D.O. Thompson and D.E. Chimenti, (Plenum, New York, 1986) p. 1449.
8. C. M. Sayers and D. R. Allen, J. Phys. D 17, 1399 (1984).
9. Y. Iwashimizu and O. Kobori, J. Acoust. Soc. Am. 64, 910 (1978).
10. P. P. Delsanto and A. V. Clark, Jr., J. Acoust. Soc. Am. 81, 952 (1987).
11. G. T. Mase and G. C. Johnson, J. Appl. Mech. 54, 126 (1987).
12. R. B. Thompson, S. S. Lee and J. F. Smith, J. Acoust. Soc. Am. 80, 921 (1986).
13. R. B. Thompson, S. S. Lee and J. F. Smith, Appl. Phys. Lett. 44, 296 (1984).
14. C.-S. Man and W. Y. Lu, J. Elasticity 17, 159 (1987).
15. T. Tokuoka and Y. Iwashimizu, Int. J. Solids Structures 4, 383 (1968).
16. Landolt-Börnstein, in *Numerical Data and Functional Relationships in Science and Technology*, Vol. III/11, (Springer, New York ,1979)
17. Y. C. Chu and S. I. Rokhlin, J. Acoust. Soc. Am. 95, 213 (1994).
18. Y. C. Chu, A. D. Degtyar and S. I. Rokhlin, J. Acoust. Soc. Am. 95, 3191 (1994).
19. S. I. Rokhlin and W. Wang, J. Acoust. Soc. Am. 92, 3303 (1992).